

Dual Inhibitors of Thymidylate Synthase and Dihydrofolate Reductase as Antitumor Agents: Design, Synthesis, and Biological Evaluation of Classical and Nonclassical Pyrrolo[2,3-*d*]pyrimidine Antifolates¹

Aleem Gangjee,^{*,†} Hiteshkumar D. Jain,[†] Jaclyn Phan,[†] Xin Lin,[†] Xiaohong Song,^{†,||} John J. McGuire,[‡] and Roy L. Kisliuk[§]

Division of Medicinal Chemistry, Graduate School of Pharmaceutical Sciences, Duquesne University, Pittsburgh, Pennsylvania 15282, Grace Cancer Drug Center, Roswell Park Cancer Institute, Elm and Carlton Streets, Buffalo, New York 14263, and Department of Biochemistry, Tufts University School of Medicine, Boston, Massachusetts 02111

Received October 20, 2005

We designed and synthesized a classical analogue *N*-[4-[(2-amino-6-ethyl-3,4-dihydro-4-oxo-7*H*-pyrrolo[2,3-*d*]pyrimidin-5-yl)thio]benzoyl]-L-glutamic acid (**4**) and thirteen nonclassical analogues **5**–**17** as potential dual thymidylate synthase (TS) and dihydrofolate reductase (DHFR) inhibitors and as antitumor agents. The key intermediate in their synthesis was 2-amino-6-ethyl-3,4-dihydro-4-oxo-7*H*-pyrrolo[2,3-*d*]pyrimidine, **22**, to which various aryl thiols were conveniently attached at the 5-position via an oxidative addition reaction using iodine. For the classical analogue **4**, the ester obtained from the reaction was deprotected and coupled with diethyl L-glutamate followed by saponification. Compound **4** was a potent dual inhibitor of human TS (IC₅₀ = 90 nM) and human DHFR (IC₅₀ = 420 nM). Compound **4** was not a substrate for human FPGS. Metabolite protection studies established TS as its principal target. Most of the nonclassical analogues were only inhibitors of human TS with IC₅₀ values of 0.23–26 μM.

Introduction

Folate metabolism has long been recognized as an attractive target for cancer chemotherapy because of its indispensable role in the biosynthesis of nucleic acid precursors.^{2,3} Within folate metabolism, thymidylate synthase (TS), which catalyzes the reductive methylation of 2'-deoxyuridine-5'-monophosphate (dUMP) to 2'-deoxythymidine-5'-monophosphate (dTMP), has been of particular interest.⁴ For this biochemical transformation, 5,10-methylenetetrahydrofolate serves as the source of the methyl group as well as the reductant and is oxidized to 7,8-dihydrofolate (7,8-DHF).⁴ For continuous production of dTMP in dividing cells, the oxidized 7,8-DHF must be converted back to 5,10-methylenetetrahydrofolate. Dihydrofolate reductase (DHFR)⁵ catalyzes the first of the two steps in this biotransformation in which NADPH acts as the source of the reductant.⁶ Thus TS and DHFR are crucial for the synthesis of dTMP in dividing cells, and hence inhibition of either leads to "thymineless death". Thus both TS and DHFR represent attractive targets for developing antitumor agents. Several TS and DHFR inhibitors, as separate entities, have found clinical utility as antitumor agents.⁷ Figure 1 illustrates important examples of clinically used TS inhibitors such as raltitrexed⁸ and pemetrexed⁹ (Figure 1). Similarly, methotrexate (MTX), a DHFR inhibitor, has been used clinically for more than 50 years.¹⁰ Generally 2,4-diaminopyrimidine containing antifolates are inhibitors of DHFR while 2-amino-4-oxopyrimidine containing antifolates are inhibitors of TS.^{11,12} Raltitrexed is a quinazoline analogue containing a 6–6 ring-fused system similar to natural folates. Pemetrexed contains a 6–5 ring-fused pyrrolo[2,3-*d*]pyrimidine system and is designated a multitargeted antifolate (MTA). Pemetrexed and its polyglutamylated metabolites are inhibitors of several important folate-dependent enzymes including TS,

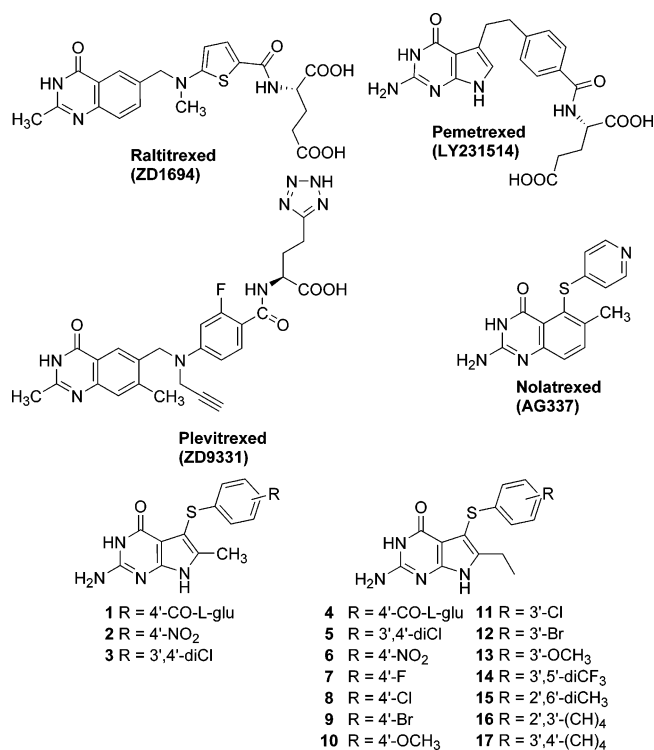


Figure 1.

DHFR, glycinamideribonucleotide formyltransferase (GARFT), and aminoimidazole carboxamideribonucleotide formyltransferase (AICARFT).^{13,14} The primary locus of action of pemetrexed is the inhibition of TS which is also responsible for its cytotoxic effects.¹⁴ However, inhibition of other folate-dependent enzymes may also be important, since pemetrexed is cytotoxic to human cancer cell lines that are resistant to raltitrexed and 5-FU as a result of TS amplification.¹⁵ Using molecular modeling, we¹⁶ suggested that pemetrexed might bind to DHFR in a "2,4-diamino mode" (Figure 2). This binding mode is

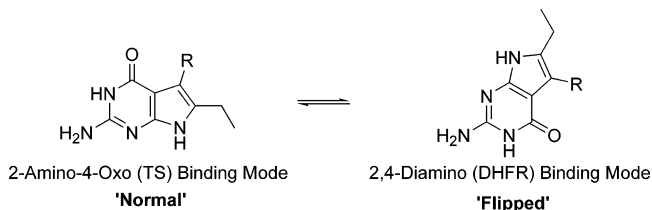
* To whom correspondence should be addressed. E-mail: gangjee@duq.edu. Phone: 412-396-6070. Fax: 412-396-5593.

[†] Duquesne University.

[‡] Roswell Park Cancer Institute.

[§] Tufts University School of Medicine.

^{||} Present address: Abbott Laboratories, Abbott Park, IL 60064.

**Figure 2.**

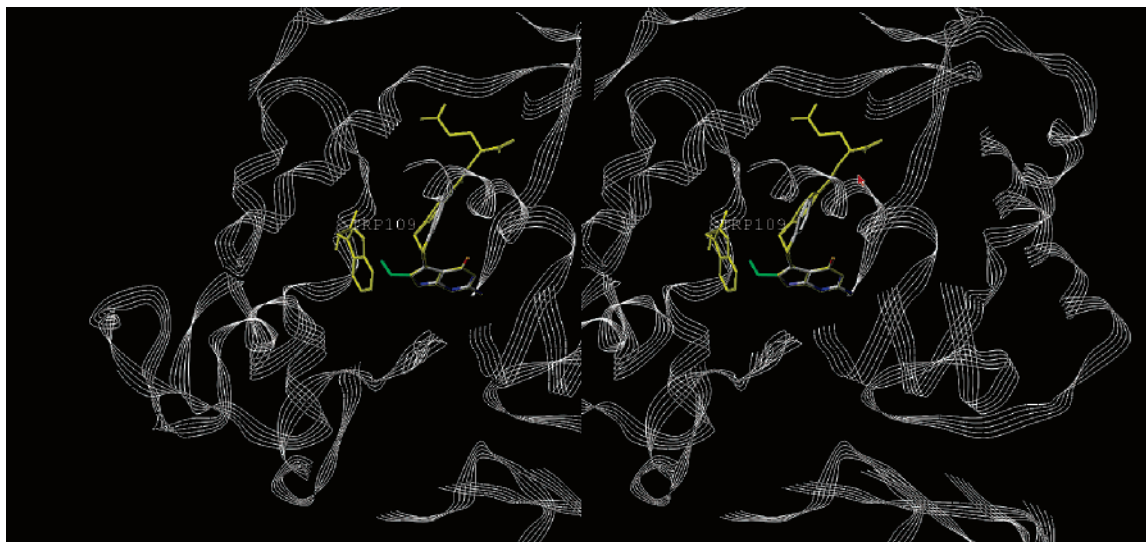
obtained on rotation of 180° about the 2-NH₂-C₂ bond in which the pyrrole nitrogen mimics the 4-amino group of MTX.¹⁶ The fact that X-ray crystal structures show that this flipped mode of binding actually occurs with 2-amino-4-methyl antifolates^{16,17} lends credence to our hypothesis.

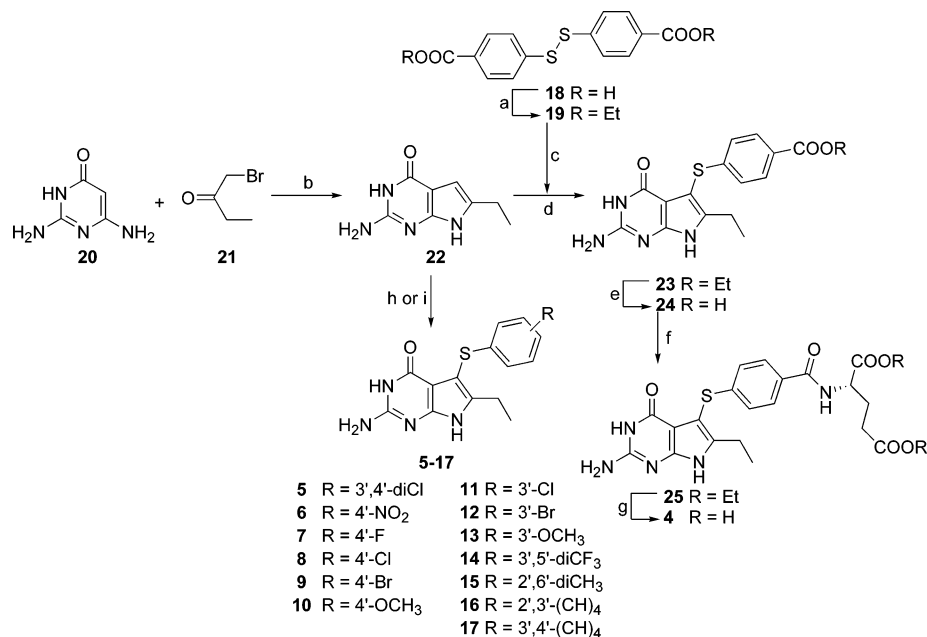
Raltitrexed and pemetrexed are good substrates for the enzyme folylpoly- γ -glutamate synthetase (FPGS).^{8,9} FPGS catalyzes the production of poly- γ -glutamates which leads to high intracellular concentrations of folates and antifolates and in some cases increases TS inhibitory activity for antifolates such as raltitrexed⁸ (60-fold) and pemetrexed⁹ (130-fold) compared to their monoglutamate forms.^{18–21} Although polyglutamylation of certain antifolates is necessary for cytotoxicity, it has also been implicated in toxicity to normal host cells due to cellular retention of the polyanionic poly- γ -glutamate metabolites which do not efflux from normal cells.²² Additionally, tumor cells develop resistance to antifolates which depend on polyglutamylation for their antitumor effects by producing low or defective FPGS and thereby limiting their use.^{36,23–26} A potential approach to circumvent drawbacks associated with FPGS, including resistance, is to design compounds that are not substrates for FPGS and yet have high antitumor activity in their monoglutamate forms. A compound not subject to activation by polyglutamylation needs to have high intrinsic potency as a TS inhibitor. One such nonpolyglutamylatable, potent TS inhibitor plevitrexed (Figure 1), is currently undergoing phase I/II clinical trial as an antitumor agent.^{27,28}

It has been our long standing goal to design and synthesize compounds that are potent dual inhibitors of TS and DHFR and that do not depend on FPGS for inhibitory potency. Such compounds would be capable of providing "combination therapy" as a single agent without the pharmacokinetic disadvantages of two separate agents. Gangjee et al.²⁹ reported a classical 2-amino-4-oxo-6-methyl-5-substituted pyrrolo[2,3-*d*]-

pyrimidine, **1**, as a potent inhibitor of human TS ($IC_{50} = 42$ nM) and a marginal inhibitor of human DHFR ($IC_{50} = 2.2$ μ M) in its monoglutamate form thus providing a dual inhibitor of human TS and human DHFR. Additionally, compound **1** was not a substrate for human FPGS at concentrations up to 1045 μ M thus indicating that **1** does not require polyglutamylation for its potent inhibition of the target enzymes. The lack of FPGS substrate activity of **1** was attributed, in part, to the presence of the 6-methyl group on the pyrrolo[2,3-*d*]pyrimidine of **1**.²⁹ Thus compound **1** is a promising lead compound which can be further modified to enhance human TS, human DHFR, and tumor cell inhibitory activity. Molecular modeling using SYBYL 6.91³⁰ indicated that compound **1** should bind to human DHFR in the "2,4-diamino mode" (Figure 2) similar to that proposed for pemetrexed,¹⁶ thereby allowing for moderate human DHFR inhibition. Additionally, molecular modeling indicated that the 6-methyl group of **1** makes hydrophobic contact with Val115 in human DHFR. This potential hydrophobic interaction with Val115 is absent in pemetrexed which does not have the 6-methyl group. We^{31,32} have long advocated and recently^{16,33} shown that dual TS-DHFR inhibitory activity in 6–5 antifolates can occur in two different binding modes one to TS and a flipped mode to DHFR. For 2-amino-4-oxo-5-substituted-6-alkyl pyrrolo[2,3-*d*]pyrimidines the two modes are shown in Figure 2. The 2-amino-4-oxo mode is proposed for TS binding and rotation about the NH₂-C₂ bond by 180° affords the flipped 2,4-diamino mode proposed for DHFR binding.

Gangjee et al.³⁴ using molecular modeling (SYBYL 6.91)³⁰ suggested that the 6-methyl group in **1** makes important hydrophobic contacts with Trp109 in human TS and also sterically restricts the rotation of the 5-position side-chain so that it adopts a favorable conformation for binding to TS. Above all, compound **1** ($EC_{50} = 0.45$ μ M) was a better inhibitor of the growth of CCRF-CEM human leukemic cells in culture than was *N*-[4-[*N*-(2-amino-3,4-dihydro-4-oxo-6-quinazolinyl)methyl]-*N*-prop-2-ynylamino]benzoyl]-L-glutamic acid (PDDF) ($EC_{50} = 0.72$ μ M), a standard TS inhibitor. Molecular modeling (SYBYL 6.91)³⁰ further indicated that the 6-methyl can be homologated to a 6-ethyl which further enhances the van der Waals interaction with Trp109 in human TS (Figure 3) in the 2-amino-4-oxo mode and Val115 in human DHFR in the flipped 2,4-diamino mode. We were aware of a minor steric hindrance between the 6-ethyl group of compound **4** and Trp109 in human TS; however, it

**Figure 3.** Stereoview compound **4** superimposed on LY231514 (not shown) in human TS (PDB code 1JU6).⁶⁴ The hydrophobic interaction between 6-ethyl and Trp109 is shown.

Scheme 1^a

^a Conditions: (a) EtI, NaHCO₃, rt, 120 h; (b) DMF, 40–50 °C, 72 h; (c) NaBH₄, EtOH, rt, 30 min; (d) I₂, EtOH/H₂O (2:1), 100–110 °C; (e) 1N NaOH, 80 °C, 24 h; (f) ^tBuOCOCl, NEt₃, diethyl L-glutamate hydrochloride, 0 °C to room temperature; (g) 1 N NaOH, 0 °C, 4 h, then rt, 20 h; (h) ArSH, I₂, EtOH/H₂O (2:1), 100–110 °C for **5–7**, **9**, **11**, **12**, **14**, and **15**; (i) ArSH, PIFA, (CF₃)₂CHOH, rt, N₂ for **8**, **10**, **13**, **16**, and **17**.

was anticipated that this would not be deleterious for the binding of **4** to human TS since the molecule could tilt sufficiently in its binding to alleviate the mild clash of the 6-ethyl group with Trp109. Thus the 6-ethyl group might decrease the TS inhibitory activity compared to **1** but was expected to enhance the DHFR inhibitory activity compared to **1**. Thus *N*-[4-[(2-amino-6-ethyl-3,4-dihydro-4-oxo-7*H*-pyrrolo[2,3-*d*]pyrimidin-5-yl)thio]-benzoyl]-L-glutamic acid, **4**, the 6-ethyl homologue of compound **1** was designed and synthesized as a potential dual inhibitor of human TS and human DHFR.

An additional problem associated with classical antifolates is their dependence on the carrier systems for their uptake into the cell. The reduced folate carrier (RFC) is most important in this regard.³⁵ Impairment of either FPGS³⁶ and/or RFC^{37–40} system(s) can lead to drug resistance. To overcome the aforementioned problems associated with classical antifolates, lipophilic nonclassical antifolates were also designed and synthesized. These lipophilic nonclassical antifolates lack the polar glutamate found in classical antifolates and hence do not have to depend on FPGS for their inhibitory activity of the target enzymes. Additionally, they do not have to depend on the RFC system for active uptake into the cell system since they are lipophilic and are passively taken up into the cells. Nolatreted (Figure 1) is the first nonclassical TS inhibitor to reach clinical trials.^{41,42}

Gangjee et al.⁴³ have shown that nonclassical analogues of **1** with electron-withdrawing groups in the phenyl ring of the side chain enhance human TS inhibitory activity. Extensive SAR studies indicated that analogues with electron withdrawing groups at both the 3'- and/or 4'-positions of the phenyl side chain provide optimum inhibitory potency against human TS. Nonclassical analogues such as **2** (IC₅₀ = 0.15 μM) and **3** (IC₅₀ = 0.13 μM) were much more potent than the clinically used raltitrexed and pemetrexed against human TS.⁴³ Electron-donating substituents such as methoxy, methyl, and bulky substituents such as naphthyl are conducive for DHFR inhibition;^{11,12} hence analogues containing these substituents were also synthesized. As indicated above for the classical **4** it was

anticipated that the 6-ethyl nonclassical analogues of **1** would also provide dual inhibitory activity. To determine the effect of 6-substituent homologation on human TS and human DHFR inhibitory activity in the nonclassical analogues, compounds **5–17** were also synthesized. The synthesis and biological activities of analogues **4–17** are presented in this report.

Chemistry

The key intermediate in the synthesis of analogues **4–17** was 2-amino-6-ethyl-3,4-dihydro-4-oxo-7*H*-pyrrolo[2,3-*d*]pyrimidine, **22** (Scheme 1), to which various side chains were conveniently attached at the 5-position via an oxidative addition reaction using iodine as reported previously.^{29,34,43} A search revealed that compound **22** was not reported in the literature. Gangjee et al.⁴⁴ had previously reported that α-bromoketones on cyclization with 2,6-diamino-4-oxopyrimidine, **20**, give 2-amino-4-oxo-6-substituted pyrrolo[2,3-*d*]pyrimidine in reasonably good yield. Thus we envisioned that compound **22** could be obtained in a single step from commercially available 1-bromo-2-butanone, **21**, and 2,6-diamino-4-oxopyrimidine, **20**. Thus⁴⁴ heating a mixture of **20** and **21** in DMF under N₂ for a period of 72 h at 40–50 °C gave **22** in a moderate 40% yield. The reaction was found to be incomplete (TLC) even after 72 h and longer reaction times resulted in decomposition of the product (TLC). Separation of pure **22** was tedious and difficult and required extensive column chromatography. Higher reaction temperatures were also found to give additional products (TLC) further complicating the purification. Reaction of **22** with appropriately substituted aryl thiols in a mixture of ethanol/water (2:1) followed by addition of I₂ at reflux as reported previously^{29,34,43} afforded the desired compounds **5**, **6**, **7**, **9**, **11**, **12**, **14**, **15** in 35–55% yields. In an attempt to circumvent the harsh reaction conditions (reflux) and to further improve the overall yield for the thiolation procedure that we have utilized thus far, an alternative thiolation procedure was tried. This method⁴⁵ involved direct nucleophilic sulfenylation of pyrrolo[2,3-*d*]pyrimidines using hypervalent iodine reagent, phenyl-iodine(III)bis(trifluoroacetate) (PIFA) in 1,1,1,3,3,3-hexafluoro-

Table 1. Inhibition of Isolated TS and DHFR

compd	TS IC ₅₀ (nM)		DHFR IC ₅₀ (μM)	
	human ^a	<i>E. coli</i> ^a	human ^b	<i>E. coli</i> ^c
1	54	270	2.1	21
2^d	150	nd	nd	nd
3^d	130	nd	nd	nd
4	90	540	0.42	>21
5	230	>2.3 × 10 ⁻⁵ (41) ^e	>27 (0)	nd
6	240	24000	>29 (33)	nd
7	2700	>2.7 × 10 ⁻⁵ (0)	>32 (0)	nd
8	>3.1 × 10 ⁻⁵ (25)	>3.1 × 10 ⁻⁵ (27)	nd	nd
9	1000	>2.2 × 10 ⁻⁵ (15)	>26 (14)	nd
10	16000	>3.2 × 10 ⁻⁵ (22)	nd	nd
11	2600	>2.6 × 10 ⁻⁵ (13)	>31 (0)	nd
12	1100	>2.3 × 10 ⁻⁵ (10)	>27 (0)	nd
13	>3.2 × 10 ⁻⁵ (15)	>3.2 × 10 ⁻⁵ (5)	nd	nd
14	>2.2 × 10 ⁻⁵ (18)	>2.0 × 10 ⁻⁵ (0)	>24 (14)	nd
15	26000	>2.6 × 10 ⁻⁵ (0)	>31 (0)	nd
16	5600	>3.0 × 10 ⁻⁵ (15)	nd	nd
17	5600	3.0 × 10 ⁻⁵	nd	nd
PDDF ^f	72	72	nd	nd
raltitrexed ^g	380	5700	nd	nd
pemetrexed ^h	9500	76000	6.6	230
MTX	nd	nd	0.022	0.0066

^a Kindly provided by Dr. Frank Maley, New York State Department of Health. ^b Kindly provided by Dr. J. H. Freisheim, Medical College of Ohio, Toledo, OH. ^c Kindly provided by Dr. R. L. Blakley, St. Jude Children's hospital, Memphis TN. ^d Data derived from ref 43; nd = not determined. ^e Numbers in parentheses indicate the % inhibition at the stated concentration. ^f Kindly provided by Dr. M. G. Nair, University of South Alabama. ^g Kindly provided by Dr. Ann Jackman, Institute of Cancer Research, Sutton, Surrey, UK. ^h Kindly provided by Dr. Chuan Shih, Eli Lilly and Co.

2-propanol [(CF₃)₂CHOH], a poorly nucleophilic and polar solvent. This reaction could be carried out under mild conditions (rt) without the necessity of heating. Thus a solution of **22** (1 equivalent), the appropriate arylthiols (2 equivalents), and PIFA (1.5 equivalents) in (CF₃)₂CHOH was stirred under N₂ at room temperature for 24 h to afford target compounds **8**, **10**, **13**, **16**, and **17** in 9–17% yields. The low yield of this reaction discouraged further utilization of this procedure. For the synthesis of the classical analogue **4**, the required disulfide, **19**, was prepared as reported previously²⁹ from commercially available 4,4'-dimercaptobis(benzoic acid), **18**. Reduction of **19** to the corresponding sodium salt of ethyl 4-mercaptobenzoate was achieved using NaBH₄ in EtOH.^{29,34} Reaction of the sodium salt of the mercaptan with the pyrrolo[2,3-*d*]pyrimidine, **22**, gave ester **23** (Scheme 1) in 44% yield.^{29,34} The structures of **5**–**17** and **23** were established by ¹H NMR where the disappearance of the 5-aryl proton at 5.87 ppm, present in **22**, and the presence of the requisite protons of the aryl side chain confirmed the required structures. Ester hydrolysis of **23** with 1N NaOH at 80 °C afforded the corresponding acid **24** in 75% yield.^{29,34} Peptide coupling^{29,34} of the acid **24** with diethyl L-glutamate using the mixed anhydride method with isobutyl chloroformate and triethylamine afforded **25** in 65% yield. The ¹H NMR spectrum of **25** in deuterated dimethyl sulfoxide revealed the expected peptide NH doublet at 8.44–8.47 ppm which exchanged on addition of D₂O. Hydrolysis of the diester **25** with aq NaOH at room temperature, followed by acidification with 3 N HCl at lowered temperatures, afforded the desired target **4** in 80% yield.

Biological Evaluation and Discussion

The classical and nonclassical analogues **4**–**17** were evaluated as inhibitors of recombinant human (rh) and *Escherichia coli* (*E. coli*) TS⁴⁶ and DHFR⁴⁷ (Table 1) and compared with PDDF (a standard TS inhibitor), raltitrexed, pemetrexed, and methotrexate (MTX). The classical analogue **4** was a potent inhibitor

of rhTS and rh DHFR. Against rhTS, analogue **4** was similar in potency to PDDF and about 2-fold less potent than the previously reported compound **1**. This result indicates that homologation of a 6-methyl to a 6-ethyl in pyrrolo[2,3-*d*]pyrimidines is marginally detrimental to rhTS inhibitory activity. This decrease in potency may be due to steric hindrance between the 6-ethyl group of **4** and Trp109 in human TS as predicted from molecular modeling and/or due to unfavorable orientation of the 5-position side chain for interaction with the human TS enzyme in the presence of the 6-ethyl moiety. Interestingly **4** was 4-fold more potent than raltitrexed and a remarkable 106-fold more than pemetrexed against rhTS. Similar results were obtained with *E. coli* TS. Analogue **4** was 6-fold more potent against human TS than *E. coli* TS, indicating a significant species difference. Compound **4** was 8-fold less potent against *E. coli* TS than PDDF but was more than 140-fold as potent as pemetrexed. Compound **4** was also a potent inhibitor of human DHFR (Table 1) and was >40-fold more potent in inhibiting human DHFR than *E. coli* DHFR. Compound **4** was 5-fold more potent than **1** and 16-fold more potent than pemetrexed as an inhibitor of rhDHFR. This increase in activity against rhDHFR, of **4** over **1**, may be attributed to increased hydrophobic interaction of the 6-ethyl moiety of **4** and Val115 in human DHFR as predicted by molecular modeling. The increased activity may also result from favorable orientation of the 5-position thioaryl side chain that is more conducive for binding to human DHFR. Interestingly **4** was only 19-fold less potent than MTX as an inhibitor of rhDHFR. These data suggest that homologation of a 6-methyl to a 6-ethyl is highly conducive to rhDHFR inhibitory activity and maintains the TS inhibitory potency, thus affording an improved dual TS-DHFR inhibitor over **1**. The nonclassical analogues **5**–**17** were also evaluated as inhibitors of TS and DHFR (Table 1). Except for **8**, **13**, and **14**, all of the nonclassical analogues were inhibitors of human TS with IC₅₀ values of 0.23–26 μM. The nonclassical analogues **5** and **6** were comparable in potency to the 6-methyl homologues, **3** and **2**, respectively, and were more potent against human TS than the clinically used classical antifolates raltitrexed and pemetrexed. Most of the nonclassical analogues were also more potent than pemetrexed as inhibitors of human TS. This result indicates that homologation of a 6-methyl to a 6-ethyl in nonclassical 6-alkylpyrrolo[2,3-*d*]pyrimidine maintains potent human TS inhibitory activity. The SAR against human TS indicates that electron withdrawing substituents (except **8** and **14**) on the side-chain phenyl ring are more conducive for human TS inhibition than electron-donating substituents. In addition bulky substituents such as 1-naphthyl (**16**) and 2-naphthyl (**17**) afford marginal activity against human TS. These data is consistent with SAR studies in the previously reported 6-methyl series. Analogues **5**–**17** were in general poor inhibitors of human DHFR, *E. coli* TS and *E. coli* DHFR (Table 1).

Growth inhibitory potency of **4** was compared to that of MTX in continuous exposure against CCRF-CEM human lymphoblastic leukemia and a series of MTX-resistant sublines (Table 2). Compound **4** was nearly 200-fold less potent than MTX at inhibiting the growth of CCRF-CEM cells in culture. The DHFR overexpressing cell line R1 was <3-fold cross-resistant to **4**, suggesting that DHFR is probably not the primary target of this analogue. The MTX-resistant transport-deficient subline R2, that does not express functional reduced folate carrier⁴⁸ (RFC), is ≈5-fold cross-resistant to **4**, while it is 120-fold cross-resistant to MTX. These data suggest that **4** utilizes the RFC as its primary means of transport into the cell, but at high extracellular levels it may be able to diffuse through the plasma membrane.

Table 2. Growth Inhibition of Parental CCRF-CEM Human Leukemia Cells and Sublines with Single, Defined Mechanisms of MTX Resistance during Continuous Exposure (0–120 h) Exposure to MTX and **4**^d

drug	EC ₅₀ , (nM)			
	CCRF-CEM	R1 ^a (↓ DHFR)	R2 ^b (↓ uptake)	R30dm ^c (↓ Glu _n)
MTX	14 ± 0	565 ± 65	1700 ± 100	17 ± 1
1 ^e	450 ± 100	nd	nd	810 ± 200
4	2700 ± 200	7050 ± 250	12500 ± 500	2900 ± 100

^a CCRF-CEM subline resistant to MTX solely as a result of a 20-fold increase in wild-type DHFR protein and activity.³⁷ ^b CCRF-CEM subline resistant as a result of decrease uptake of MTX.³⁸ ^c CCRF-CEM subline resistant to MTX solely as a result of decreased polyglutamylation; this cell line has 1% of the FPGS specific activity (measured with MTX as the folate substrate) of parental CCRF-CEM.¹⁶ ^d Values presented are average ± range for *n* = 2. ^e Data derived from ref 29.

Table 3. Protection of CCRF-CEM Human Leukemia Cells against the Growth Inhibitory Effects of MTX or **4** by 10 μM Hypoxanthine (Hx), 5 μM Thymidine (TdR), and Their Combination

drug	relative growth (%) ^{a,b}			
	no addition	5 μM TdR	10 μM Hx	Hx + TdR
MTX (40 nM)	10 ± 1	10 ± 0	11 ± 0	99 ± 1
4 (15000 nM)	18 ± 0	106 ± 3	16 ± 1	105 ± 3

^a Deoxycytidine (dCyd; 10 μM) was present in all the above cultures to prevent the inhibition of growth caused in T-cell leukemias such as CCRF-CEM by TdR (see experimental). In typical results, dCyd alone had no effect on CCRF-CEM growth (100 ± 3% of control) and did not protect against growth inhibition by either drug (data not shown). Hx alone (101 ± 3% of control) or in the presence of dCyd (102 ± 3% of control) did not affect CCRF-CEM growth and did not protect against MTX-induced growth inhibition (Table above). TdR alone inhibited growth of CCRF-CEM (44 ± 2% of control), but TdR+dCyd was essentially not growth inhibitory (101 ± 2% of control) and neither protected against MTX-induced growth inhibition (Table above). Similarly, Hx+TdR+dCyd was only slightly inhibitory to growth of CCRF-CEM (87 ± 1% of control). ^b Growth is expressed relative to quadruplicate cultures not treated with either drug or metabolite and is the average ± range for duplicate treated samples. The experiment was repeated with similar results.

Thus the reason for the decreased CCRF-CEM inhibitory activity of compound **4** relative to **1** could be that it is more poorly transported into CCRF-CEM cells. A subline (R30dm) expressing low levels of foylpolypoly-γ-glutamate synthetase (FPGS) is not cross-resistant to **4** under continuous exposure conditions suggesting that polyglutamate forms of **4** are not essential to its mechanisms of action.

Metabolite protection studies were performed to further elucidate the mechanism of action of **4** and are shown in Table 3. At a concentration of MTX that inhibited growth of CCRF-CEM cells by 95%, leucovorin at 0.1 μM was able to fully protect against the effects of MTX (10 ± 4% growth inhibition). In contrast, at a concentration of **4** that inhibited growth by 95%, even 10 μM leucovorin only afforded marginal protection (75 ± 0% growth inhibition). Although this might suggest that **4** is not an antifolate, some validated antifolates (e.g., BW1843U89⁴⁹) are poorly protected by leucovorin. These data do suggest, however, that leucovorin “rescue”, as used clinically with high-dose MTX,⁵⁰ would not be successful with **4**. Further studies in CCRF-CEM cells examined the ability of thymidine (TdR) and/or hypoxanthine (Hx) to protect against growth inhibition. These metabolites can be salvaged to produce dTTP and the purine dNTPs required for DNA synthesis and thus bypass the MTX blockade.⁵¹ As described in the Experimental Section, in T-lymphoblast cell lines such as CCRF-CEM, TdR can only be tested in the presence of deoxycytidine (dCyd), which reverses its toxic effects; however, dCyd has no protective effect on MTX either alone or in paired combination with either Hx

Table 4. Activity of Folate Analogue as Substrates for Recombinant Human FPGS^a

substrate	K _m , μM	V _{max,rel} ^b	V _{max,rel} /K _m	<i>n</i>
AMT	6.5 ± 0.6	1.00	0.15	2
4	inactive ≤ 100 μM	0	0	2

^a FPGS substrate activity was determined as described in Experimental Section. Values presented are the average ± SD. ^b V_{max,rel} is calculated based on the apparent V_{max} of a substrate relative to the apparent V_{max} of AMT within the same experiment.

or TdR (Table 3; footnote). The data (Table 3) show that for **4**, TdR alone protects against growth inhibition, while Hx alone does not; addition of Hx to TdR does not affect the protection. These data suggest that **4** inhibits only thymidylate synthesis, indicating that TS is the target of this drug. Thus the one-carbon homologated analogue has the same mechanism of action as its methylated parent **1**.

The substrate activity of **4** with recombinant human FPGS was evaluated in vitro and, compared to that of AMT, a good substrate for FPGS. The data (Table 4) show that **4** is a very poor substrate for human FPGS at up to 100 μM (at 100 μM, **4** has ≤3% of the activity exhibited by 40 μM AMT). The lack of FPGS substrate activity is consistent with the lack of cross-resistance of the FPGS-deficient subline R30dm (above) to **4** and underscores the absence of a requirement for polyglutamylation for the cytotoxicity of **4**. These data also further substantiate the idea that methyl and ethyl substituents in the 6-position of classical pyrrolo[2,3-d]pyrimidines and in the 7-position of quinazolines⁵² prevent FPGS substrate activity as a consequence of bulk and/or hydrophobicity which is not tolerated by human FPGS.

Molecular Modeling

In an attempt to explain the superior human DHFR inhibitory activity of compound **4** over its congener **1**, a docking study using GOLD 2.2^{53–55} was performed. In this study, the 1.9 Å X-ray crystal structure of human DHFR complexed with MTX and NADPH (PDB entry 1U72)⁵⁶ was chosen as the human DHFR standard. The binding site was defined by the cocrystallized ligand MTX with the default setting, which for the active site definition, is all protein atoms within 5.0 Å of each ligand atom plus the atoms of their associated residues.

The Goldscore-CS docking protocol⁵³ was adopted in this study. In this protocol, the poses obtained with the original Goldscore function are rescored and reranked with the GOLD implementation of the Chemscore function.^{53,57} To perform a thorough and unbiased search of the conformation space, each docking run was allowed to produce 30 poses without the option of early termination.

To test the validity of this protocol for the human DHFR system, MTX, the cocrystallized ligand, was first docked back into its binding site. In this docking run, the 30 poses produced by GOLD could be divided into two clusters on the basis of their conformations: twelve of the poses closely resembled the cocrystallized conformation with a heavy atom root-mean-square deviation (RMSD) ranging from 0.68 to 1.34 Å, while the remaining eighteen poses roughly adopted the “flipped conformation” with a heavy atom RMSD varying between 1.8 and 2.1 Å. Chemscore was able to rank eight out of the twelve poses from the first cluster as the highest ranked eight poses (Figure 4). Thus this docking protocol was considered to be suitable for the subsequent docking runs for compounds **1** and **4**.

Both compounds **1** and **4** were docked as described above for MTX. In both cases, 29 of 30 poses, which included the highest ranked pose, adopted the “flipped conformation”. The

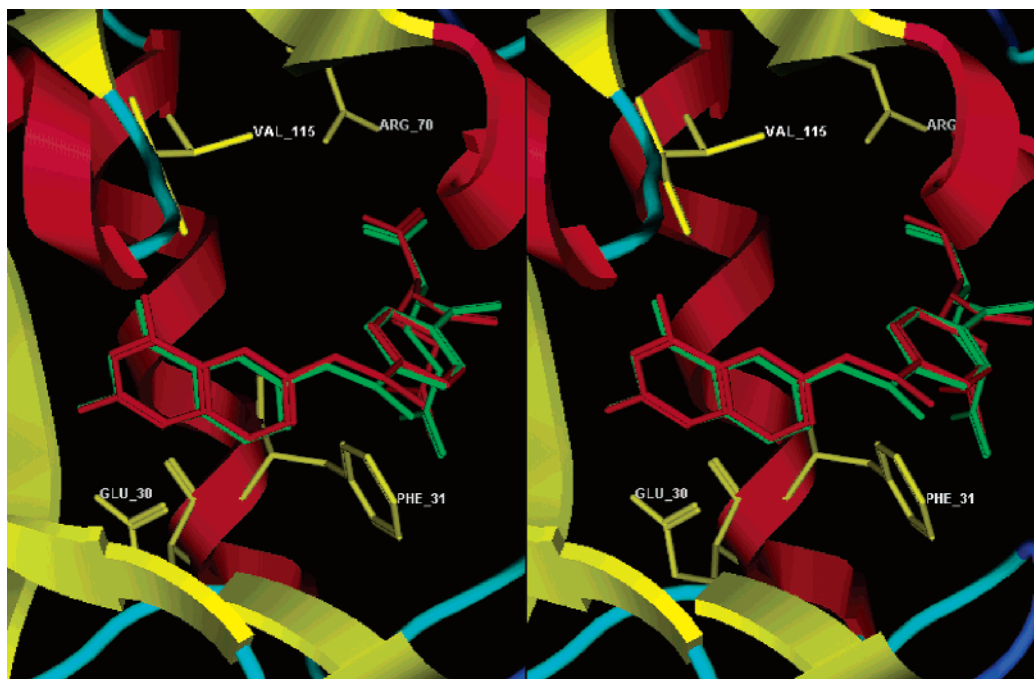


Figure 4. Comparison of the crystallized MTX (red) and the docked MTX (green) in the binding site of human DHFR (PDB code 1U72).⁵⁶

Table 5. Binding Energy Calculated by Chemscore

compd	$\Delta G_{\text{binding}}$ (kJ/mol)	ΔG_{hbond} (kJ/mol)	ΔG_{lipo} (kJ/mol)	ΔS (kJ/mol)	ΔE_{clash} (kJ/mol)	ΔE_{int} (kJ/mol)
1	-25.51	-14.73	-19.82	10.74	2.58	1.2
4	-27.39	-13.56	-22.03	11.10	0.89	1.69

free energy of binding for the highest ranked pose for compound **1** and **4** according to Chemscore⁵³ is listed in Table 5. The highest ranked poses of MTX, **1** and **4** were compared in Figure 5.

Chemscore calculates the free energy of binding with the following formula:⁵³

$$\Delta G_{\text{binding}} = -5.48 + \Delta G_{\text{hbond}} + \Delta G_{\text{lipo}} + \Delta S + \Delta E_{\text{clash}} + \Delta E_{\text{int}}$$

where ΔG_{hbond} , ΔG_{lipo} are hydrogen-bonding and lipophilic interaction respectively, ΔS represents the loss of conformational entropy of the ligand upon binding to the receptor, and ΔE_{clash} and ΔE_{int} are the protein–ligand clash-energy and ligand–internal-energy, respectively. Chemscore also considers acceptor–metal and covalently bound ligand energy terms, these terms are not applicable to the human DHFR system and are omitted from this formula.

According to this calculation, by homologating the 6-methyl group to an ethyl, compound **4** lost 1.17 kJ/mol in hydrogen-bonding, 0.36 kJ/mol in entropy, 0.49 kJ/mol in internal energy but gained 2.2 kJ/mol in lipophilic interaction and 1.69 kJ/mol in protein–ligand clashing energy. Overall, compound **4** gained 1.87 kJ/mol in the free energy of binding, which corresponds to 2.12-fold difference in affinity compared to **1**.

A possible explanation for the loss of hydrogen-bonding and gain in protein–ligand clashing energy for compound **4** is that the bulkier 6-ethyl group might restrain the 5-side-chain to some extent and provide a conformation which affords less hydrogen-bonding but also fewer steric clashes between compound **4** and the active site. The fact that compound **4** has a slightly higher ligand internal energy (0.49 kJ/mol higher) supports the above hypothesis. The difference in hydrophilic interaction is appar-

ently due to the extra carbon at the 6-position, which according to the docking study interacts with the alkyl side chain of Val115 (Figure 6). Finally, since compound **4** has one extra carbon, it has a higher degree of freedom than compound **1**; thus it will also suffer a greater entropy loss upon binding.

In summary, homologation of a 6-methyl (compound **1**) to a 6-ethyl (compound **4**) in 2-amino-4-oxo-5-thiobenzoyl-6-alkyl-pyrrolo[2,3-*d*]pyrimidine increases the human DHFR inhibitory activity while maintaining the human TS inhibitory activity, thus providing an improved dual human TS and human DHFR inhibitor. Thus we have shown that in classical *N*-[4-[(2-amino-6-alkyl-3,4-dihydro-4-oxo-7*H*-pyrrolo[2,3-*d*]pyrimidin-5-yl)-thio]-benzoyl]-L-glutamic acid containing analogues dual TS-DHFR activity can be obtained by 6-alkyl substitution. The fact that homologated 6-alkyl substituents such as ethyl are well tolerated by human TS coupled with increased DHFR inhibitory activity indicates that further homologation of the 6-alkyl group may be possible and will be the subject of future communications. Docking study revealed that both compounds **1** and **4** will most possibly adopt the “flipped” binding mode when complexed with human DHFR. It also suggested that the 6-ethyl group not only interacts with Val115 but may also control the conformation of the 5-side chain. Compound **4** is 6-fold less potent than the parent analogue **1** as an inhibitor of CCRF-CEM cell growth. Cross-resistance and metabolite protection data corroborate a similar mechanism of action for **1** and **4**. Both compounds **1** and **4** target TS directly. Interestingly leucovorin does not afford complete protection against **1** or **4**. Neither analogue is a substrate for human FPGS, and hence polyglutamates are not critical to their mechanism of action. This lack of substrate activity of compound **4** can be an important attribute to overcome potential resistance to classical TS inhibitors such as raltitrexed and pemetrexed which depend on intracellular polyglutamylolation to exert their cytotoxic effects. Nonclassical homologated ethyl analogues **5** and **6** were also potent inhibitors of human TS similar to the methyl analogues **2** and **3**. These nonclassical analogues were also more potent inhibitors of human TS than pemetrexed or raltitrexed in their monoglutamate forms.

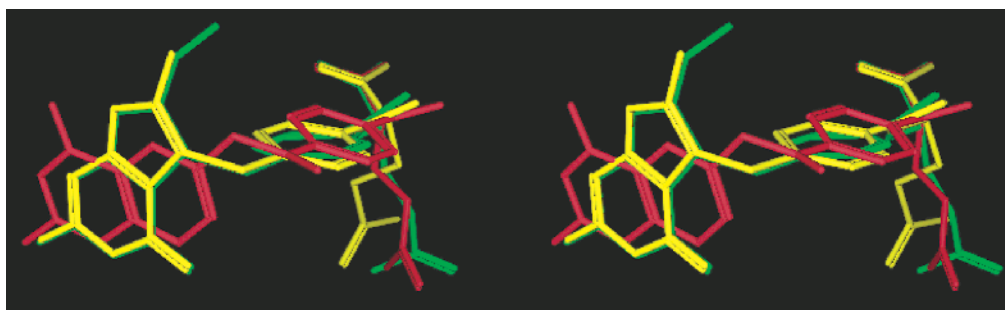


Figure 5. A comparison of the highest ranked poses of MTX (red), compound **1** (yellow), and **4** (green).

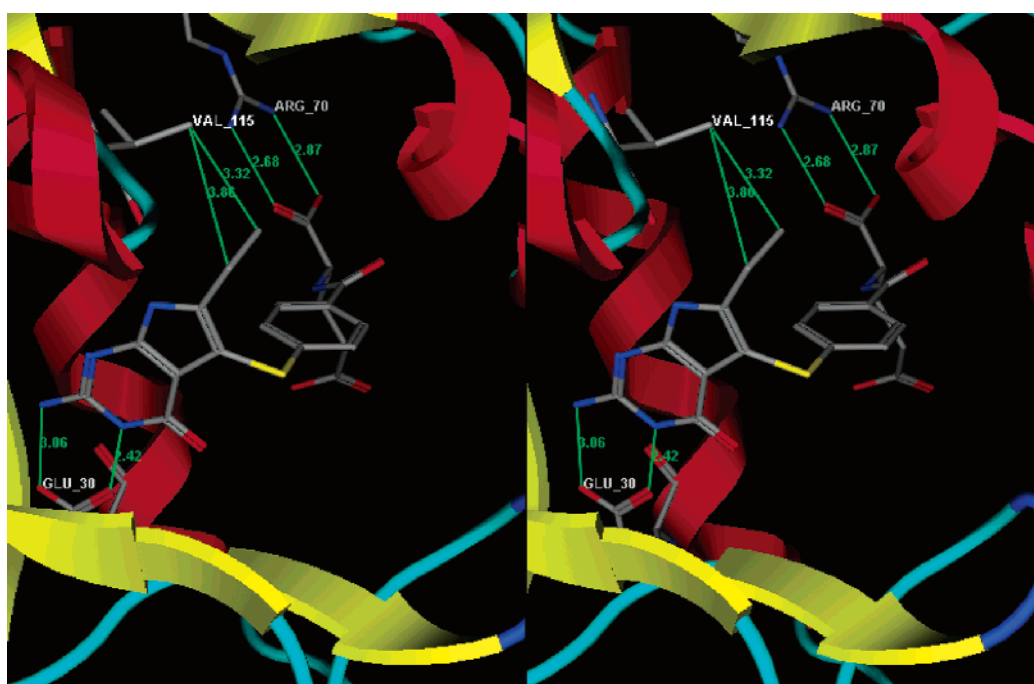


Figure 6. Possible interaction between compound **4** and human DHFR based on its docking result. Arg70 and Glu30 interact with the α -carboxy group of the glutamate moiety and 2-NH₂/3-NH group, respectively, and are shown in the figure as reference residues. The hydrophobic interaction between 6-ethyl and Val115 is shown.

Experimental Section

All evaporations were carried out in vacuo with a rotary evaporator. Analytical samples were dried in vacuo (0.2 mmHg) in an Chem-Dry vacuum-drying oven apparatus over P₂O₅. Melting points were determined on a MEL-TEMP II melting point apparatus and are uncorrected. Nuclear magnetic resonance spectra for proton (¹H NMR) were recorded on a Bruker WH-300 (300 MHz) spectrometer. Chemical shift values are expressed in ppm (parts per million) relative to tetramethylsilane as the internal standard; s = singlet, d = doublet, dd = doublet of doublets, t = triplet, q = quartet, m = multiplet, bs = broad singlet. The relative integrals of peak areas agreed with those expected for the assigned structures. Mass spectra were recorded on a VG-7070 double-focusing mass spectrometer or in a LKB-9000 instrument in the electron ionization (EI) mode. Thin-layer chromatography (TLC) was performed on Polygram Sil G/UV₂₅₄ silica gel plates with fluorescent indicator, and the spots were visualized under 254 and 366 nm illumination. Proportions of solvents used for TLC are by volume. Elemental analyses were performed by Atlantic Microlabs Inc., Norcross, GA. Analytical results indicated by element symbols are within $\pm 0.4\%$ of calculated values. Fractional moles of water or organic solvents frequently found in some analytical samples of antifolates could not be removed despite 24–48 h of drying in vacuo and were confirmed where possible by their presence in the ¹H NMR spectrum. All solvents and chemicals were purchased from Aldrich Chemical Co. and Fisher Scientific and were used as received.

2-Amino-6-ethyl-3,4-dihydro-4-oxo-7H-pyrrolo[2,3-*d*]pyrimidine (22). A mixture of 2,6-diamino-4-oxypyrimidine (**20**) (4.18 g, 33.1 mmol), 1-bromo-2-butanone (**21**) (5.00 g, 33.1 mmol), and DMF (20 mL) was heated between 40 and 50 °C under N₂ for 72 h. At this time silica gel (30 g) was added and the solvent was evaporated to dryness (oil pump) to afford a silica gel plug, which was loaded on a wet (CHCl₃) silica gel column and eluted initially with CHCl₃ (500 mL) and then sequentially with 500 mL of 5%, 10%, 15%, and 20% MeOH in CHCl₃. Fractions that showed the major spot at R_f 0.37 were pooled and evaporated to dryness. EtOAc was added to the resulting residue and the mixture filtered. The collected solid was recrystallized using methanol to afford 2.6 g (40%) of **22** as a light pink solid; mp 251–258 °C; TLC R_f 0.37 (CHCl₃/MeOH, 5:1, with 2 drops of concentrated NH₄OH); ¹H NMR (DMSO-*d*₆) δ 1.13–1.17 (t, 3 H, 6-CH₂CH₃), 2.45–2.50 (q, 2 H, 2-CH₂CH₃), 5.87 (s, 1 H, 5-CH), 6.17 (s, 2 H, 2-NH₂), 10.29 (s, 1 H, 3-NH), 10.90 (s, 1 H, 7-NH).

2-Amino-6-ethyl-5-[(3',4'-dichlorophenyl)sulfanyl]-3,4-dihydro-4-oxo-7H-pyrrolo[2,3-*d*]pyrimidine (5). To a solution of **22** (0.7 g, 3.93 mmol) in a mixture of ethanol/water (3:2, 40 mL) was added 3,4-dichlorothiophenol (1.4 g, 7.86 mmol), and the reaction mixture was heated to 100–110 °C. At this time I₂ (2.0 g, 8.0 mmol) was added and the heating continued with stirring for a total of 3 h. To this mixture was added excess Na₂S₂O₇, and the mixture was concentrated under reduced pressure. To the resulting residue was added 5 g of silica gel and MeOH, and the solution was evaporated

to dryness to afford a dry silica gel plug which was loaded on top of a wet (CHCl₃) silica gel column and eluted with a gradient of 1–5% MeOH in CHCl₃. Fractions containing the desired spot (TLC) were pooled and evaporated to dryness. The resulting residue was recrystallized from MeOH, filtered, and dried to yield 0.670 g (48%) of **5** as a pale white solid: mp 252–257 °C; TLC *R_f* 0.49 (CHCl₃/MeOH, 5:1, with 2 drops of concentrated NH₄OH); ¹H NMR (DMSO-*d*₆) δ 1.06–1.11 (t, 3 H, 6-CH₂CH₃), 2.56–2.63 (q, 2 H, 2-CH₂CH₃), 6.16 (s, 2 H, 2-NH₂), 6.95–6.98 (d, 1 H, C₆H₄), 7.17 (s, 1 H, C₆H₃), 7.43–7.46 (d, 1 H, C₆H₃), 10.26 (s, 1 H, 3-NH), 11.53 (s, 1 H, 7-NH). Anal. Calcd for (C₁₄H₁₂N₄SOCl₂·0.5H₂O) C, H, N, S, Cl.

2-Amino-6-ethyl-5-[(4'-nitrophenyl)sulfanyl]-3,4-dihydro-4-oxo-7H-pyrrolo[2,3-*d*]pyrimidine (6). Compound **6** (synthesized as described for **5**): yield 55%; mp 215–220 °C; TLC *R_f* 0.45 (CHCl₃/MeOH, 5:1, with 2 drops of concentrated NH₄OH); ¹H NMR (DMSO-*d*₆) δ 1.06–1.10 (t, 3 H, 6-CH₂CH₃), 2.56–2.64 (q, 2 H, 6-CH₂CH₃), 5.61 (s, 2 H, 2-NH₂), 7.17–7.20 (d, 2 H, C₆H₄), 8.03–8.06 (d, 2 H, C₆H₄), 10.78 (s, 1 H, 7-NH), 11.89 (s, 1 H, 3-NH). Anal. Calcd for (C₁₄H₁₃N₅O₃S·1.0H₂O) C, H, N, S.

2-Amino-6-ethyl-5-[(4'-fluorophenyl)sulfanyl]-3,4-dihydro-4-oxo-7H-pyrrolo[2,3-*d*]pyrimidine (7). Compound **7** (synthesized as described for **5**): yield 50%; mp 300–304.7 °C; TLC *R_f* 0.44 (CHCl₃/MeOH, 5:1, with 2 drops of concentrated NH₄OH); ¹H NMR (DMSO-*d*₆) δ 1.05–1.10 (t, 3 H, 6-CH₂CH₃), 2.57–2.64 (q, 2 H, 2-CH₂CH₃), 6.10 (s, 2 H, 2-NH₂), 7.04–7.07 (d, 4 H, C₆H₄), 10.20 (s, 1 H, 3-NH), 11.41 (s, 1 H, 7-NH). Anal. Calcd for (C₁₄H₁₃N₄OSF·0.5H₂O) C, H, N, S, F.

2-Amino-6-ethyl-5-[(4'-chlorophenyl)sulfanyl]-3,4-dihydro-4-oxo-7H-pyrrolo[2,3-*d*]pyrimidine (8). To a stirred solution of **22** (154.3 mg, 0.87 mmol) in (CF₃)₂CHOH (2 mL) was added 6 drops of 4-chlorothiophenol and PIFA (613.4 mg, 1.43 mmol), and the reaction mixture was stirred under N₂ at room temperature for 24 h. Solvent was removed under reduced pressure. To the resulting residue was added 0.5 g silica gel and MeOH (10 mL), and the solution was evaporated to dryness to afford a dry silica gel plug which was loaded on top of a wet (CHCl₃) silica gel column and eluted first with CHCl₃ and then with a gradient of 1–5% MeOH in CHCl₃. Fractions containing the desired spot (TLC) were pooled and evaporated to dryness. The resulting residue was recrystallized from MeOH, filtered, and dried to yield 24 mg (9%) of **8** as a pale white solid: mp 252–257 °C; TLC *R_f* 0.49 (CHCl₃/MeOH, 5:1, with 2 drops of concentrated NH₄OH); ¹H NMR (DMSO-*d*₆) δ 1.04–1.09 (t, 3 H, 6-CH₂CH₃), 2.57–2.60 (q, 2 H, 2-CH₂CH₃), 6.14 (s, 2 H, 2-NH₂), 6.98–7.01 (d, 2 H, C₆H₄), 7.23–7.26 (d, 2 H, C₆H₄), 10.24 (s, 1 H, 3-NH), 11.47 (s, 1 H, 7-NH). Anal. Calcd for (C₁₄H₁₃N₄O) MS (EI) Calc *m/z* = 320.0499 Found *m/z* = 320.0501 (M⁺)

2-Amino-6-ethyl-5-[(4'-bromophenyl)sulfanyl]-3,4-dihydro-4-oxo-7H-pyrrolo[2,3-*d*]pyrimidine (9). Compound **9** (synthesized as described for **5**): yield 40%; mp 301–306 °C; TLC *R_f* 0.45 (CHCl₃/MeOH, 5:1, with 2 drops of concentrated NH₄OH); ¹H NMR (DMSO-*d*₆) δ 1.07 (t, 3 H, 6-CH₂CH₃), 2.57 (q, 2 H, 6-CH₂CH₃), 6.11 (s, 2 H, 2-NH₂), 6.91–6.94 (d, 2 H, C₆H₄), 7.36–7.38 (d, 2 H, C₆H₄), 10.22 (s, 1 H, 7-NH), 11.46 (s, 1 H, 3-NH). Anal. Calcd for (C₁₄H₁₃N₄OSBr·1.0H₂O) C, H, N, S, Br.

2-Amino-6-ethyl-5-[(4'-methoxyphenyl)sulfanyl]-3,4-dihydro-4-oxo-7H-pyrrolo[2,3-*d*]pyrimidine (10). Compound **10** (synthesized as described for **8**): yield 12%; mp 215–220 °C; TLC *R_f* 0.45 (CHCl₃/MeOH, 5:1, with 2 drops of concentrated NH₄OH); ¹H NMR (DMSO-*d*₆) δ 1.07 (t, 3 H, 6-CH₂CH₃), 2.63 (q, 2 H, 6-CH₂CH₃), 3.68 (s, 3 H, 4'-OCH₃), 6.08 (s, 2 H, 2-NH₂), 6.81 (d, 2 H, C₆H₄), 7.05 (d, 2 H, C₆H₄), 10.18 (s, 1 H, 7-NH), 11.32 (s, 1 H, 3-NH). Anal. Calcd for (C₁₅H₁₆N₄O₂S) MS (EI) Calc *m/z* = 316.0994 Found *m/z* = 316.0981 (M⁺)

2-Amino-6-ethyl-5-[(3'-chlorophenyl)sulfanyl]-3,4-dihydro-4-oxo-7H-pyrrolo[2,3-*d*]pyrimidine (11). Compound **11** (synthesized as described for **5**): yield 46%; mp 282–288 °C; TLC *R_f* 0.51 (CHCl₃/MeOH, 5:1, with 2 drops of concentrated NH₄OH); ¹H NMR (DMSO-*d*₆) δ 1.06–1.10 (t, 3 H, 6-CH₂CH₃), 2.59–2.61 (q, 2 H, 2-CH₂CH₃), 6.14 (s, 2 H, 2-NH₂), 6.95–6.99 (m, 2 H, C₆H₄),

7.11 (s, 1 H, C₆H₄), 7.21–7.26 (t, 1 H, C₆H₄), 10.26 (s, 1 H, 3-NH), 11.50 (s, 1 H, 7-NH). Anal. Calcd for (C₁₄H₁₃N₄O) MS (EI) C, H, N, S, Cl.

2-Amino-6-ethyl-5-[(3'-bromophenyl)sulfanyl]-3,4-dihydro-4-oxo-7H-pyrrolo[2,3-*d*]pyrimidine (12). Compound **12** (synthesized as described for **5**): yield 40%; mp 249–255 °C; TLC *R_f* 0.56 (CHCl₃/MeOH, 5:1, with 2 drops of concentrated NH₄OH); ¹H NMR (DMSO-*d*₆) δ 1.06–1.11 (t, 3 H, 6-CH₂CH₃), 2.56–2.61 (q, 2 H, 2-CH₂CH₃), 6.15 (s, 2 H, 2-NH₂), 7.00–7.02 (d, 1 H, C₆H₄), 7.10 (s, 1 H, C₆H₄), 7.14–7.25 (m, 2 H, C₆H₄), 10.26 (s, 1 H, 3-NH), 11.50 (s, 1 H, 7-NH). Anal. Calcd for (C₁₄H₁₃N₄OSBr·0.2H₂O) C, H, N, S, Br.

2-Amino-6-ethyl-5-[(3'-methoxyphenyl)sulfanyl]-3,4-dihydro-4-oxo-7H-pyrrolo[2,3-*d*]pyrimidine (13). Compound **13** (synthesized as described for **8**): yield 16%; mp 249–255 °C; TLC *R_f* 0.56 (CHCl₃/MeOH, 5:1, with 2 drops of concentrated NH₄OH); ¹H NMR (DMSO-*d*₆) δ 1.06–1.11 (t, 3 H, 6-CH₂CH₃), 2.56–2.61 (q, 2 H, 2-CH₂CH₃), 6.15 (s, 2 H, 2-NH₂), 7.00–7.02 (d, 1 H, C₆H₄), 7.10 (s, 1 H, C₆H₄), 7.14–7.25 (m, 2 H, C₆H₄), 10.26 (s, 1 H, 3-NH), 11.50 (s, 1 H, 7-NH). Anal. Calcd for (C₁₅H₁₆N₄O₂S) MS (EI) Calc *m/z* = 316.0994 Found *m/z* = 316.0990 (M⁺)

2-Amino-6-ethyl-5-[(3',5'-trifluoromethylphenyl)sulfanyl]-3,4-dihydro-4-oxo-7H-pyrrolo[2,3-*d*]pyrimidine (14). Compound **14** (synthesized as described for **5**): yield 35%; mp 290–294.5 °C; TLC *R_f* 0.47 (CHCl₃/MeOH, 5:1, with 2 drops of concentrated NH₄OH); ¹H NMR (DMSO-*d*₆) δ 1.06–1.10 (t, 3 H, 6-CH₂CH₃), 2.57–2.65 (q, 2 H, 2-CH₂CH₃), 6.19 (s, 2 H, 2-NH₂), 7.61 (s, 2 H, C₆H₃), 7.75 (s, 1 H, C₆H₃), 10.34 (s, 1 H, 3-NH), 11.62 (s, 1 H, 7-NH). Anal. Calcd for (C₁₆H₁₂N₄OSF₆) C, H, N, S, F.

2-Amino-6-ethyl-5-[(2',6'-dimethylphenyl)sulfanyl]-3,4-dihydro-4-oxo-7H-pyrrolo[2,3-*d*]pyrimidine (15). Compound **15** (synthesized as described for **5**): yield 35%; mp 290–294.5 °C; TLC *R_f* 0.47 (CHCl₃/MeOH, 5:1, with 2 drops of concentrated NH₄OH); ¹H NMR (DMSO-*d*₆) δ 1.06–1.10 (t, 3 H, 6-CH₂CH₃), 2.57–2.65 (q, 2 H, 2-CH₂CH₃), 6.19 (s, 2 H, 2-NH₂), 7.61 (s, 2 H, C₆H₃), 7.75 (s, 1 H, C₆H₃), 10.34 (s, 1 H, 3-NH), 11.62 (s, 1 H, 7-NH). Anal. Calcd for (C₁₆H₁₂N₄OSF₆) C, H, N, S, F.

2-Amino-6-ethyl-5-[(1'-naphthyl)sulfanyl]-3,4-dihydro-4-oxo-7H-pyrrolo[2,3-*d*]pyrimidine (16). Compound **16** (synthesized as described for **8**): yield 10%; mp 249–255 °C; TLC *R_f* 0.56 (CHCl₃/MeOH, 5:1, with 2 drops of concentrated NH₄OH); ¹H NMR (DMSO-*d*₆) δ 1.04–1.09 (t, 3 H, 6-CH₂CH₃), 2.57–2.64 (q, 2 H, 2-CH₂CH₃), 6.12 (s, 2 H, 2-NH₂), 6.83–6.86 (d, 1 H, C₁₀H₇), 7.29–7.32 (d, 1 H, C₁₀H₇), 7.55–7.66 (m, 3 H, C₁₀H₇), 7.90–7.93 (d, 1 H, C₁₀H₇), 8.24–8.26 (d, 1 H, C₁₀H₇), 10.24 (s, 1 H, 3-NH), 11.51 (s, 1 H, 7-NH). Anal. Calcd for (C₁₈H₁₆N₄O) MS (EI) Calc *m/z* = 336.1045 Found *m/z* = 336.1054 (M⁺)

2-Amino-6-ethyl-5-[(2'-naphthyl)sulfanyl]-3,4-dihydro-4-oxo-7H-pyrrolo[2,3-*d*]pyrimidine (17). Compound **17** (synthesized as described for **8**): yield 17%; mp 249–255 °C; TLC *R_f* 0.56 (CHCl₃/MeOH, 5:1, with 2 drops of concentrated NH₄OH); ¹H NMR (DMSO-*d*₆) δ 1.07–1.11 (t, 3 H, 6-CH₂CH₃), 2.62–2.65 (q, 2 H, 2-CH₂CH₃), 6.13 (s, 2 H, 2-NH₂), 7.22 (d, 1 H, C₁₀H₇), 7.41 (m, 2 H, C₁₀H₇), 7.68–7.81 (m, 3 H, C₁₀H₇), 8.05 (s, 1 H, C₁₀H₇), 10.22 (s, 1 H, 3-NH), 11.48 (s, 1 H, 7-NH). Anal. Calcd for (C₁₈H₁₆N₄O) MS (EI) Calc *m/z* = 336.1045 Found *m/z* = 336.1049 (M⁺)

Ethyl 4-[(2-Amino-6-ethyl-3,4-dihydro-4-oxo-7H-pyrrolo[2,3-*d*]pyrimidin-5-yl)sulfanyl]benzoate (23). To a solution of 4,4'-dithiobis(benzoic acid), **18** (4.59 g, 25 mmol), in anhydrous *N,N*-dimethylacetamide (25 mL) was added powdered NaHCO₃ (5.04 g, 60 mmol) followed by EtI (9.36 g, 60 mmol), and the reaction mixture was stirred under N₂ for 120 h. The mixture was then diluted with water (50 mL) and extracted with EtOAc (3 × 100 mL). The combined organic layer was washed with water (50 mL) and brine (50 mL) and then dried (MgSO₄) and filtered. The filtrate was evaporated to a dark brown oil under reduced pressure. This oil was chromatographed on a wet (CH₂Cl₂) silica gel column and eluted with CH₂Cl₂. Fractions containing the desired spot (TLC) were pooled and evaporated to dryness to afford **19** as a tan oil that was used immediately in the next step. To a solution of **19** (2.2 g, 6 mmol) in absolute EtOH (20 mL) was added NaBH₄ (0.23

g, 6 mmol) all at once and the mixture stirred under N₂ for 30 min. To this ethanolic solution of the sodium salt of ethyl 4-mercapto-benzoate was added **22** (0.53 g, 3 mmol), the ratio of ethanol/water was adjusted to 3/2 (40 mL), and the resulting suspension was heated to 100 °C. At this time I₂ (1.5 g, 6 mmol) was added and the resulting solution was refluxed for 4 h, when TLC indicated the disappearance of starting material at R_f 0.37 and the formation of a major spot at R_f 0.50 (CHCl₃/MeOH 5:1, with 2 drops of concentrated NH₄OH). To the resulting solution was added excess Na₂S₂O₃, and the reaction mixture was evaporated to dryness. To the resulting residue was added silica gel (10 g) and MeOH, and the solvent was evaporated under low pressure to give a plug which was chromatographed on silica gel using a gradient of 1–5% MeOH in CHCl₃. Fractions containing the desired spot (TLC) were pooled and evaporated to dryness to afford 470 mg (44%) of **23** as a light cream solid: mp 228–234 °C; TLC R_f = 0.50 (CHCl₃/MeOH 5:1, with 2 drops of concentrated NH₄OH); ¹H NMR (DMSO-*d*₆) δ 1.05–1.10 (t, 3 H, 6-CH₂CH₃), 1.26–1.30 (t, 3 H, COOCH₂CH₃), 2.53–2.59 (q, 2 H, 6-CH₂CH₃), 4.25–4.29 (q, 2 H, COOCH₂CH₃), 6.15 (s, 2 H, 2-NH₂), 7.05–7.08 (d, 2 H, C₆H₄), 7.75–7.78 (d, 2 H, C₆H₄), 10.26 (s, 1 H, 7-NH), 11.53 (s, 1 H, 7-NH).

Diethyl N-[4-[(2-Amino-6-ethyl-3,4-dihydro-4-oxo-7H-pyrrolo[2,3-d]pyrimidin-5-yl)thio]benzoyl]-L-glutamate (25). To a solution of **23** (400 mg, 1.1 mmol) in ethanol (40 mL) was added aqueous 1 N NaOH, and the reaction mixture was heated at 80 °C for 16 h. The solution was evaporated to dryness, and the sodium salt was dissolved in water (20 mL) and carefully acidified to pH 4 by dropwise addition of 3 N HCl. The resulting suspension was left at 0 °C for 24 h and filtered. The residue was washed with water, ethyl acetate, and diethyl ether and dried over P₂O₅ at 78 °C to afford 277 mg (75%) of the free acid **24** as a light brown solid. To a suspension of the acid **24** (250 mg, 0.75 mmol) in anhydrous DMF (15 mL) under N₂ was added triethylamine (270 μL, 1.9 mmol), and the suspension was stirred under N₂ at room temperature to form a solution. This solution was cooled to 0 °C and isobutyl chloroformate (270 μL, 2.0 mmol) was added, followed 15 min later by diethyl L-glutamate hydrochloride (0.48 g, 2.0 mmol) and immediately followed by triethylamine (270 μL, 2.0 mmol). The reaction mixture was slowly allowed to warm to room temperature and stirred for 24 h. The DMF was evaporated using an oil pump at room temperature. To the resulting residue was added 25 mL of methanol and silica gel (2 g) and the suspension was evaporated to dryness. The silica gel plug was loaded on a wet (CHCl₃) silica gel column and eluted with a gradient of 1–5% MeOH in CHCl₃. Fractions containing the desired spot (TLC) were pooled and evaporated to dryness under vacuum to give 260 mg (65%) of **25** as a light cream solid: mp 198–202 °C; TLC R_f = 0.52 (CHCl₃/MeOH 5:1, with 2 drops of concentrated NH₄OH); ¹H NMR (DMSO-*d*₆) δ 1.07–1.10 (t, 3 H, 6-CH₂CH₃), 1.13–1.17 (t, 6 H, COOCH₂CH₃), 1.14–1.21 (m, 6 H, CH₂CH₃), 1.97–2.08 (m, 2 H, Glu β-CH₂), 2.38–2.41 (t, 2 H, Glu γ-CH₂), 2.57–2.59 (q, 2 H, 6-CH₂CH₃), 4.00–4.10 (q, 4 H, COOCH₂CH₃), 4.39 (m, 1 H, Glu α-CH), 6.11 (s, 2 H, 2-NH₂), 7.02–7.04 (d, 2 H, C₆H₄), 7.67–7.70 (d, 2 H, C₆H₄), 8.55–8.58 (d, 1 H, CONH), 10.22 (s, 1 H, 7NH), 11.48 (s, 1 H, 3NH). Anal. Calcd for (C₂₄H₂₉N₅SO₆·0.5H₂O) C, H, N, S

N-[4-[(2-Amino-6-ethyl-3,4-dihydro-4-oxo-7H-pyrrolo[2,3-d]pyrimidin-5-yl)thio]-benzoyl]-L-glutamate Acid (4). To a solution of **25** (200 mg, 0.38 mmol) in ethanol (5 mL) was added 1 N NaOH (1 mL), and the solution was stirred at 0 °C (4 h) and then at room temperature for 24 h. The ethanol was evaporated under reduced pressure, the residue was dissolved in water (5 mL), and the solution was stirred for a further 24 h. The solution was then cooled in an ice-bath and acidified carefully to pH 4.0 with dropwise addition of 3 N HCl. This suspension was left at 5 °C for 24 h and filtered. The residue was washed well with water and ether and dried over P₂O₅ /vacuum to afford 140 mg (80%) of **4** as a light cream solid: mp 214–220 °C; TLC R_f = 0.60 (CHCl₃/MeOH/NH₄OH 3:9:1); ¹H NMR (DMSO-*d*₆) δ 1.05–1.10 (t, 3 H, 6-CH₂CH₃), 1.93–2.08 (m, 2 H, Glu β-CH₂), 2.31–2.35 (t, 2 H, Glu γ-CH₂), 2.55–2.60 (q, 2 H, 6-CH₂CH₃), 4.35 (m, 1 H, Glu α-CH), 6.15 (s, 2 H, 2-NH₂),

7.02–7.05 (d, 2 H, C₆H₄), 7.68–7.71 (d, 2 H, C₆H₄), 8.44–8.47 (d, 1 H, CONH), 10.26 (s, 1 H, 7NH), 11.50 (s, 1 H, 3NH), 12.42 (bs, 2 H, COOH). Anal. Calcd for (C₂₀H₂₁N₅SO₆·1.5H₂O) C, H, N, S

Drugs and Chemicals. Drug solutions were standardized using extinction coefficients. The extinction coefficients were determined for **4** (pH 1, λ_{max} 280 nm (23600); pH 7, λ_{max} 274 nm (24000); pH 13, λ_{max} 280 nm (26400)). Extinction coefficients for methotrexate (MTX), a gift of Immunex (Seattle, WA), were from the literature.⁵⁸ Aminopterin, hypoxanthine (Hx), thymidine (TdR), and deoxycytidine (dCyd) were purchased from Sigma Chemical Co. (St. Louis, MO). Calcium leucovorin (LV) was purchased from Schircks Laboratories (Jona, Switzerland). Other chemicals and reagents were reagent grade or higher.

Cell Lines and Methods for Measuring Growth Inhibitory Potency. Cell lines were verified to be negative for Mycoplasma contamination (Mycoplasma Plus PCR primers, Stratagene, La Jolla, CA). The human T-lymphoblastic leukemia cell line CCRF-CEM⁵⁹ and its MTX-resistant sublines R1,⁶⁰ R2,⁶¹ and R30dm²⁵ were cultured as described.²⁵ R1 expresses 20-fold elevated levels of dihydrofolate reductase (DHFR), the target enzyme of MTX. R2 has dramatically reduced MTX uptake, but normal levels of MTX-sensitive DHFR. R30dm expresses 1% of the folypolyglutamate synthetase (FPGS) activity of CCRF-CEM and is resistant to short-term, but not continuous, MTX exposure; however, R30dm is cross-resistant in continuous exposure to antifolates that require polyglutamylation to form potent inhibitors. Growth inhibition of all cell lines by continuous drug exposure was assayed as described.²⁵ ⁴⁹ EC₅₀ values (drug concentration effective at inhibiting cell growth by 50%) were determined visually from plots of percent growth relative to a solvent-treated control culture versus the logarithm of drug concentration.

Protection against growth inhibition of CCRF-CEM cells was assayed by including leucovorin ((6*R,S*)-5-formyltetrahydrofolate) at 0.1–10 μM with a concentration of drug previously determined to inhibit growth by 90–95%; the remainder of the assay was as described. Growth inhibition was measured relative to the appropriate leucovorin-treated control; leucovorin, even at 10 μM, caused no growth inhibition in the absence of drug, however. Protection against growth inhibition of CCRF-CEM cells was also assayed by including Hx (10 μM), TdR (5 μM), or dCyd (10 μM) individually, in pairs (Hx+dCyd, TdR+dCyd), or all together (Hx+TdR+dCyd) with concentrations of MTX or **4** that would inhibit growth by 80–90% over a growth period of ≈72 h; horse serum was decreased to 5% (normally 10%) in these studies to reduce its contribution of metabolites. The growth period was limited, because beyond 72 h CCRF-CEM cells deplete TdR in the growth media and drug effects are no longer protected. dCyd is added only to alleviate the growth inhibitory effects of 5 μM TdR against CCRF-CEM cells.⁶² Controls with metabolites alone (no drug) in the combinations described above (in duplicate), controls with drug alone with no metabolites (in duplicate), and untreated controls with neither drugs nor metabolites (in quadruplicate) were performed. Growth inhibition was measured as percent growth relative to untreated control cells (absence of drugs and metabolites).

Folypolyglutamate Synthetase (FPGS) Purification and Assay. Recombinant human cytosolic FPGS was purified and assayed as described previously.⁶³ Analogue **4** (88% recovery) was itself nearly quantitatively recovered during the assay procedure, thus ensuring that its polyglutamate products would also be quantitatively recovered. Kinetic constants for substrates were determined by the hyperbolic curve fitting subroutine of SigmaPlot (Jandel) or Kaleidagraph (Synergy Software) using a ≥10-fold range of substrate concentration. Activity was linear with respect to time at the highest and lowest AMT concentrations tested. Assays contained ≈400 units of FPGS activity; one unit of FPGS catalyzes incorporation of 1 pmol of [³H]glutamate/h.

Acknowledgment. This work was supported, in part, by grants from the National Institutes of Health, NCI (CA89300

(A.G.); CA43500 (J.M.); CA10914 (R.L.K.)) and by a Roswell Park Cancer Institute Core Grant CA16065. The authors thank Mr. William Haile for performing growth inhibition studies and FPGS activity assays.

Supporting Information Available: Results from elemental analyses. This material is available free of charge via the Internet at <http://pubs.acs.org>.

References

- Presented in part at the 227th American Chemical Society National Meeting, Anaheim, CA, March 28–April 1, 2004; Abstr. MEDI-76.
- Kisliuk, R. L. The Biochemistry of Folates. In *Folate Antagonists as Therapeutic Agents*; Sirotnak, F. M., Burchall, J. J., Ensminger, W. D., Montgomery, J. A., Eds.; Academic Press: New York, 1984; pp 1–68.
- Berman, E. M.; Werbel, L. M. The Renewed Potential for Folate Antagonists in Contemporary Cancer Chemotherapy. *J. Med. Chem.* **1991**, *34*, 479–485.
- Carreras, C. W.; Santi, D. V. Catalytic Mechanism and Structure of Thymidylate Synthase. *Ann. Rev. Biochem.* **1995**, *64*, 721–762.
- Blakley, R. L. Eukaryotic Dihydrofolate Reductase. *Adv. Enzymol. Mol. Biol.* **1995**, *70*, 23–102.
- MacKenzie, R. E. Biogenesis and Interconversion of Substituted Tetrahydrofolates. In *Folates and Pterins Chemistry and Biochemistry*; Blakley, R. L., Benkovic, S. J., Eds.; Wiley: New York, 1984; Vol. I, pp 255–306.
- Takimoto, C. H. Antifolates in Clinical Development. *Semin. Oncol.* **1997**, *24*, S18–40/S18–51.
- Jackman, A. L.; Taylor, G. A.; Gibson, W.; Kimbell, R.; Brown, M.; Calvert, A. H.; Judson, I. R.; Hughes, L. R. ICI D1694, A Quinazoline Antifolate Thymidylate Synthase Inhibitor That is a Potent Inhibitor of L1210 Tumour Cell Growth *In Vitro* and *In Vivo*: A New Agent for Clinical Study. *Cancer Res.* **1991**, *51*, 5579–5586.
- Taylor, E. C.; Kuhnt, D.; Shih, C.; Rinzel, S. M.; Grindey, G. B.; Barredo, J.; Jannatipour, M.; Moran, R. A Dideazatetrahydrofolate Analogue Lacking a Chiral Center at C-6, *N*-[4-[2-(2-Amino-3,4-dihydro-4-oxo-7H-pyrrolo[2,3-d]pyrimidin-5-yl)ethylbenzoyl]-L-glutamic Acid, Is an Inhibitor of Thymidylate Synthase. *J. Med. Chem.* **1992**, *35*, 4450–4454.
- Bertino, J. R.; Kamen, B.; Romanini, A. Folate Antagonists. In *Cancer Medicine*; Holland, J. F., Frei, E., Bast, R. C., Kufe, D. W., Morton, D. L., Weichselbaum, R. R., Eds.; Williams & Wilkins; Baltimore, MD, 1997; Vol. 1, pp 907–921.
- Rosowsky, A. Chemistry and Biological Activity of Antifolates. In *Progress in Medicinal Chemistry*; Ellis, G. P., West, G. B., Eds.; Elsevier Science: New York, 1989; Vol. 26, pp 1–252.
- Gangjee, A.; Elzein, E.; Kothare, M.; Vasudevan, A. Classical and Nonclassical Antifolates as Potential Antitumor, Antipneumocystis and Antitoxoplasma Agents. *Curr. Pharm. Des.* **1996**, *2*, 263–280.
- Mendelsohn, L. G.; Shih, C.; Chen, V. J.; Habeck, L. L.; Gates, S. B.; Shackelford, K. A. Enzyme Inhibition, Polyglutamation, and the Effect of LY231514 (MTA) on Purine Biosynthesis. *Semin. Oncol.* **1999**, *26*, 42–47.
- Shih, C.; Chen, V. J.; Gossett, L. S.; Gates, S. B.; Mackellar, W. C.; Habeck, L. L.; Shackelford, K. A.; Mendelsohn, L. G.; Soose, D. J.; et al. LY231514, a Pyrrolo[2,3-d]pyrimidine-based Antifolate that Inhibits Multiple Folate-requiring Enzymes *N*-[4-[2-(2-amino-3,4-dihydro-4-oxo-7H-pyrrolo[2,3-d]pyrimidin-5-yl)-ethyl]-benzoyl]-L-glutamic Acid (LY231514) is a novel Pyrrolo[2,3-d]pyrimidine-based Antifolate Currently Undergoing Extensive Phase II Clinical Trials. *Cancer Res.* **1997**, *57*, 1116–1123.
- Schultz, R. M.; Patel, V. F.; Worzalla, J. F.; Shih, C. Role of Thymidylate Synthase in the Antitumor Activity of the Multitargeted Antifolate, LY231514. *Anticancer Res.* **1999**, *19*, 437–443.
- Gangjee, A.; Yu, J.; McGuire, J. J.; Cody, V.; Galitsky, N.; Kisliuk, R. L.; Queener, S. F. Design, Synthesis, and X-ray Crystal Structure of a Potent Dual Inhibitor of Thymidylate Synthase and Dihydrofolate Reductase as an Antitumor Agent. *J. Med. Chem.* **2000**, *43*, 3837–3851.
- Kuyper, L. F.; Garvey, J. M.; Baccanari, D. P.; Champness, J. N.; Stammers, D. K.; Beddell, C. R. Pyrrolo[2,3-d]pyrimidines and Pyrido[2,3-d]pyrimidines as Conformationally Restricted Analogs of the Antibacterial Agent Trimethoprim. *Bioorg. Med. Chem.* **1996**, *4*, 593–602.
- Sikora, E.; Jackman, A. L.; Newell, D. F.; Calvert, A. H. Formation and Retention and Biological Activity of *N*¹⁰-Propargyl-5,8-dideazafolic Acid (CB 3717) Polyglutamates in L1210 Cells. *In Vitro. Biochem. Pharmacol.* **1988**, *37*, 4047–4054.
- Jackman, A. L.; Newell, D. R.; Gibson, W.; Jodrell, D. I.; Taylor, G. A.; Bishop, J. A.; Hughes, L. R.; Calvert, A. H. The Biochemical Pharmacology of the Thymidylate Synthase Inhibitor 2-Desamino-2-methyl-*N*¹⁰-propargyl-5,8-dideazafolic Acid (ICI 198583). *Biochem. Pharmacol.* **1991**, *41*, 1885–1895.
- Nair, M. G.; Abraham, A.; McGuire, J. J.; Kisliuk, R. L.; Galivan, J. Polyglutamylation as a Determinant of Cytotoxicity of Classical Folate Analogue Inhibitors of Thymidylate Synthase and Glycinamide Ribonucleotide Formyltransferase. *Cell. Pharmacol.* **1994**, *1*, 245–249.
- Bisset, G. M. F.; Pawelczak, K.; Jackman, A. L.; Calvert, A. H.; Hughes, L. R. Syntheses and Thymidylate Synthase Inhibitory Activity of the Poly- γ -glutamyl Conjugates of *N*-[5-[*N*-(3,4-dihydro-2-methyl-4-oxoquinazolin-6-ylmethyl)-*N*-methylamino]-2-thienoyl]-L-glutamic Acid (ICI D1694) and Other Quinazoline Antifolates. *J. Med. Chem.* **1992**, *35*, 859–866.
- Bisset, G. M. F.; Bavetsias, V.; Thornton, T. J.; Pawelczak, K.; Calvert, A. H.; Hughes, L. R.; Jackman, A. L. The Synthesis and Thymidylate Synthase Inhibitory Activity of L- γ -L-Linked Dipeptide and L- γ -Amide Analogues of 2-Desamino-2-methyl-*N*¹⁰-propargyl-5,8-dideazafolic acid (ICI 198583). *J. Med. Chem.* **1994**, *37*, 3294–3302.
- Jackman, A. L.; Kelland, L. R.; Kimbell, R.; Brown, M.; Gibson, W.; Aherne, W.; Hardcastle, A.; Boyle, F. T. Mechanisms of Acquired Resistance to the Quinazoline Thymidylate Synthase Inhibitor ZD1694 (Tomudex) in One Mouse and Three Human Cell Lines. *Br. J. Cancer.* **1995**, *71*, 914–924.
- Barakat, R. R.; Li, W. W.; Lovelace, C.; Bertino, J. R. Intrinsic Resistance of Squamous Cell Carcinoma Cell Lines as a Result of Decreased Accumulation of Intracellular Methotrexate Polyglutamates. *Gynecol. Oncol.* **1993**, *51*, 54–60.
- McCloskey, D. E.; McGuire, J. J.; Russell, C. A.; Rowan, B. G.; Bertino, J. R.; Pizzorno, G.; Mini, E. Decreased Folylpolylglutamate Synthetase Activity as a Mechanism of Methotrexate Resistance in CCRF-CEM Human Leukemia Sublines. *J. Biol. Chem.* **1991**, *266*, 6181–6187.
- Braakhuis, B. J.; Jansen, G.; Noordhuis, P.; Kegel, A.; Peters, G. J. Importance of Pharmacodynamics in the *In Vitro* Antiproliferative Activity of the Antifolates Methotrexate and 10-EDAM Against Head and Neck Squamous Cell Carcinoma. *Biochem. Pharmacol.* **1993**, *46*, 2155–2161.
- Jackman, A. L.; Kimbell, R.; Aherne, G. W.; Brunton, L.; Jansen, G.; Stephens, T. C.; Smith, M. N.; Wardleworth, J. M.; Boyle, F. T. Cellular Pharmacology and *In Vivo* Activity of a New Anticancer Agent, ZD9331: A Water-soluble, Nonpolyglutamatable, Quinazoline-Based Inhibitor of Thymidylate Synthase. *Clin. Cancer Res.* **1997**, *3*, 911–921.
- Benepal, T. S.; Judson, I. ZD9331: Discovery to Clinical Development. *Anti-Cancer Drugs* **2005**, *16*, 1–9.
- Gangjee, A.; Devraj, R.; McGuire, J. J.; Kisliuk, R. L. 5-Arylthio Substituted 2-Amino-4-oxo-6-methylpyrrolo[2,3-d]pyrimidine Antifolates as Thymidylate Synthase Inhibitors and Antitumor Agents. *J. Med. Chem.* **1995**, *38*, 4495–4502.
- Triplos Inc., 1699 South Hanley Road, St. Louis, MO, 63144.
- Gangjee, A.; Devraj, R.; McGuire, J. J.; Kisliuk, R. L.; Queener, S. F.; Barrows, L. R. Classical and Nonclassical Furo[2,3-d]pyrimidines as Novel Antifolates: Synthesis and Biological Activities. *J. Med. Chem.* **1994**, *37*, 1169–1176.
- Gangjee, A.; Devraj, R.; McGuire, J. J.; Kisliuk, R. L. Effect of Bridge Region Variation on Antifolate and Antitumor Activity of Classical 5-substituted 2,4-diaminofuro[2,3-d]pyrimidines. *J. Med. Chem.* **1995**, *38*, 3798–3805.
- Gangjee, A.; Lin, X.; McGuire, J. J.; Kisliuk, R. L. Synthesis of *N*-[4-[(2,4-diamino-5-methyl-4,7-dihydro-3H-pyrrolo[2,3-d]pyrimidin-6-yl)thio]benzoyl]-L-glutamic Acid and *N*-[4-[(2-amino-4-oxo-5-methyl-4,7-dihydro-3H-pyrrolo[2,3-d]pyrimidin-6-yl)thio]benzoyl]-L-glutamic Acid as Dual Inhibitors of Dihydrofolate Reductase and Thymidylate Synthase, and as Potential Antitumor Agents. *J. Med. Chem.* **2005**, *48*, 7215–7222.
- Gangjee, A.; Jain, H. D.; McGuire, J. J.; Kisliuk, R. L. Benzoyl Ring Halogenated Classical 2-Amino-6-methyl-3,4-dihydro-4-oxo-5-substitutedthiobenzoyl-7H-pyrrolo[2,3-d]pyrimidine Antifolates as Inhibitors of Thymidylate Synthase and as Antitumor Agents. *J. Med. Chem.* **2004**, *47*, 6730–6739.
- Cao, W.; Matherly, L. H. Structural Determinants of Folate and Antifolate Membrane Transport by the Reduced Folate Carrier. In *Drug Metabolism and Transport*; Lash, L. H., Ed.; Humana Press: Totowa, NJ, 2005; pp 291–318.
- Liani, E.; Rothem, L.; Bunni, M. A.; Smith, C. A.; Jansen, G.; Assaraf, Y. G. Loss of Folylpolyl- γ -glutamate Synthetase Activity is a Dominant Mechanism of Resistance to Polyglutamylated-dependent Novel Antifolates in Multiple Human Leukemia Sublines. *Int. J. Cancer* **2003**, *103*, 587–599.

- (37) Fry, D. W.; Jackson, R. C. Membrane Transport Alterations as a Mechanism of Resistance to Anticancer Agents. *Cancer Surv.* **1986**, *5*, 47–49.
- (38) Schornagel, J. H.; Pinard, M. F.; Westerhof, G. R.; Kathmann, I.; Molthoff, C. F. M.; Jolivet, J.; Jansen, G. Functional Aspects of Membrane Folate Receptors expressed in Human Breast Cancer Lines with Inherent and Acquired Transport-Related Resistance to Methotrexate. *Proc. Am. Assoc. Cancer Res.* **1994**, *35*, 302.
- (39) Nair, M. G.; Galivan, J.; Maley, F.; Kisliuk, R. L.; Ferone, R. Transport, Inhibition of Tumor Cell Growth and Unambiguous Synthesis of 2-Desamino-2-methyl- N^{10} -propargyl-5,8-dideazafolate (DMPDDF) and Related Compounds. *Proc. Am. Assoc. Cancer Res.* **1989**, *30*, 476.
- (40) Jackman, A. L.; Gibson, W.; Brown, M.; Kimbell, R.; Boyle, F. T. The Role of the Reduced Folate Carrier and Metabolism to Intracellular Polyglutamates for the Activity of ICI D1694. *Adv. Exp. Med. Biol.* **1993**, *339*, 265–276.
- (41) Webber, S. E.; Bleckman, T. M.; Attard, J.; Deal, J. G.; Katherdekar, V.; Welsh, K. M.; Webber, S.; Janson, C. A.; Matthews, D. A.; Smith, W. W.; Freer, S. T.; Jordan, S. R.; Bacquet, R. J.; Howland, E. F.; Booth, C. J. L.; Ward, R. W.; Hermann, S. M.; White, J.; Morse, C. A.; Hilliard, J. A.; Bartlett, C. A. Design of Thymidylate Synthase Inhibitors Using Protein Crystal Structures: The Synthesis and Biological Evaluation of a Novel Class of 5-Substituted Quinazolines. *J. Med. Chem.* **1993**, *36*, 733–746.
- (42) Hughes, A.; Calvert, A. H. Preclinical and Clinical Studies with the Novel Thymidylate Synthase Inhibitor Nolatrexed Dihydrochloride (Thymitaq, AG337). In *Antifolate Drugs in Cancer Therapy*; Jackman, A. L., Ed.; Humana Press: Totowa, NJ, 1999; pp 229–241.
- (43) Gangjee A.; Mavandadi F.; Kisliuk R. L.; McGuire J. J.; Queener S. F. 2-Amino-4-oxo-5-substituted-pyrrolo[2,3-d]pyrimidines as Non-classical Antifolate Inhibitors of Thymidylate Synthase. *J. Med. Chem.* **1996**, *39*, 4563–4568.
- (44) Gangjee, A.; Yang, J.; Ihnat, M. A.; Kamat, S. Antiangiogenic and antitumor agents. Design, synthesis, and evaluation of novel 2-amino-4-(3-bromoanilino)-6-benzyl substituted pyrrolo[2,3-d]pyrimidines as inhibitors of receptor tyrosine kinases. *Bioorg. Med. Chem.* **2003**, *11*, 5155–5170.
- (45) Kita, Y.; Takada, T.; Mihara, S.; Whelan, B. A.; Tohma, H. Novel and Direct Nucleophilic Sulfenylation and Thiocyanation of Phenol Ethers Using a Hypervalent Iodine(III) Reagent. *J. Org. Chem.* **1995**, *60*, 7144–7148.
- (46) Wahba, A. J.; Friedkin, M. The Enzymatic Synthesis of Thymidylate. Early Steps in the Purification of Thymidylate Synthetase of *Escherichia coli*. *J. Biol. Chem.* **1962**, *237*, 3794–3801.
- (47) Kisliuk, R. L.; Strumpf, D.; Gaumont, Y.; Leary, R. P.; Plante, L. Diastereoisomers of 5,10-Methylene-5,6,7,8-tetrahydropteroyl-*D*-glutamic Acid. *J. Med. Chem.* **1977**, *20*, 1531–1533.
- (48) Wong, S. C.; Zhang, L.; Witt, T. L.; Proefke, S. A.; Bhushan, A.; Matherly, L. H. Impaired Membrane Transport in Methotrexate-Resistant CCRF-CEM Cells Involves Early Translation Termination and Increased Turnover of a Mutant Reduced Folate Carrier. *J. Biol. Chem.* **1999**, *274*, 10388–10394.
- (49) McGuire, J. J.; Magee, K. J.; Russell, C. A.; Canestrari, J. M. Thymidylate Synthase as a Target for Growth Inhibition in Methotrexate Sensitive and –Resistant Human Head and Neck Cancer and Human Leukemia Cell Lines. *Oncol. Res.* **1997**, *9*, 139–147.
- (50) Bertino, J. R. Rescue Techniques in Cancer Chemotherapy: Use of Leucovorin and Other Rescue Agents after Methotrexate Treatment. *Semin. Oncol.* **1977**, *4*, 203–216.
- (51) Hakala, M. T.; Taylor, E. The Ability of Purine and Thymine Derivatives and of Glycine to Support the Growth of Mammalian Cells in Culture. *J. Biol. Chem.* **1959**, *234*, 126–128.
- (52) Marsham, P. R.; Jackman, A. L.; Barker, A. J.; Boyle, F. T.; Pegg, S. J.; Wardleworth, J. M.; Kimbell, R.; O'Connor, B. M.; Calvert, A. H.; Hughes, L. R. Quinazoline Antifolate Thymidylate Synthase Inhibitors: Replacement of Glutamic Acid in the C2-Methyl Series. *J. Med. Chem.* **1995**, *38*, 994–1004.
- (53) Verdonk, M. L.; Cole, J. C.; Hartshorn, M. J.; Murray, C. W.; Taylor, R. D. Improved Protein–Ligand Docking Using GOLD. *Proteins: Struct., Funct., Genet.* **2003**, *52*, 609–623.
- (54) Jones, G.; Willett, P.; Glen, R. C.; Leach, A. R.; Taylor, R. Development and Validation of a Genetic Algorithm for Flexible Docking. *J. Mol. Biol.* **1997**, *267*, 727–748.
- (55) Jones, G.; Willett, P.; Glen, R. C. Molecular Recognition of a Receptor Sites Using a Genetic Algorithm with a Description of Desolvation. *J. Mol. Biol.* **1995**, *245*, 43–53.
- (56) Cody, V.; Luft, J. R.; Pangborn, W. Understanding the Role of Leu22 Variants in Methotrexate Resistance: Comparison of Wild-Type and Leu22Arg Variant Mouse and Human Dihydrofolate Reductase Ternary Crystal Complexes with Methotrexate and NADPH. *Acta Crystallogr., Sect. D* **2005**, *61*, 147–155.
- (57) Eldridge, M. D.; Murray, C. W.; Auton, T. R.; Paolini, G. V.; Mee, R. P. Empirical Scoring Functions: I. The Development of a Fast Empirical Scoring Function to Estimate the Binding Affinity of Ligands in Receptor Complexes. *J. Comput.-Aided Mol. Des.* **1997**, *11*, 425–445.
- (58) Blakley, R. L. *The Biochemistry of Folic acid and Related Pteridines*; Elsevier: Amsterdam, 1969; p 569.
- (59) Foley, G. F.; Lazarus, H.; Farber, S.; Uzman, B. G.; Boone, B. A.; McCarthy, R. E. Continuous Culture of Lymphoblasts from Peripheral Blood of a Child with Acute Leukemia. *Cancer* **1965**, *18*, 522–529.
- (60) Mini, E.; Srimatkandada, S.; Medina, W. D.; Moroson, B. A.; Carman, M. D.; Bertino, J. R. Molecular and Karyological Analysis of Methotrexate-Resistant and –Sensitive Human Leukemic CCRF-CEM Cells. *Cancer Res.* **1985**, *45*, 317–325.
- (61) Rosowsky, A.; Lazarus, H.; Yuan, G. C.; Beltz, W. R.; Mangini, L.; Abelson, H. T.; Modest, E. J.; Frei, E.; III Effects of Methotrexate Esters and Other Lipophilic Antifolates on Methotrexate-Resistant Human Leukemic Lymphoblasts. *Biochem. Pharmacol.* **1980**, *29*, 648–652.
- (62) Grindey, G. B.; Wang, M. C.; Kinahan, J. J. Thymidine Induced Perturbations in Ribonucleoside Triphosphate Pools in Human Leukemic CCRF-CEM Cells. *Mol. Pharmacol.* **1979**, *16*, 601–606.
- (63) Gangjee, A.; Yu, J.; Kisliuk, R. L.; Haile, W. H.; Sobrero, G.; McGuire, J. J. Design, Synthesis, and Biological Activities of Classical *N*-{4-[2-(2-Amino-4-ethylpyrrolo[2,3-d]pyrimidin-5-yl)ethyl]benzoyl}-*L*-glutamic Acid and Its 6-Methyl Derivative as Potential Dual Inhibitors of Thymidylate Synthase and Dihydrofolate Reductase and as Potential Antitumor Agents. *J. Med. Chem.* **2003**, *46*, 591–600.
- (64) Sayre, P. H.; Finer-Moore, J. S.; Fritz, T. A.; Biermann, D.; Gates, S. B.; MacKellar, W. C.; Patel, V. F.; Stroud, R. M. Multi-targeted Antifolates Aimed at Avoiding Drug Resistance Form Covalent Closed Inhibitory Complexes with Human and *Escherichia coli* Thymidylate Synthases. *J. Mol. Biol.* **2001**, *313*, 813–829.

JM058276A